Analyst

PAPER

View Article Online
View Journal | View Issue

Open Access Article. Published on 04 September 2015. Downloaded on 10/28/2025 2:43:01 AM.
This article is licensed under a Creative Commons Attribution-NonCommercial 3.0 Unported Licence.

Cite this: *Analyst*, 2015, **140**, 7254

Label-free detection of *Phytophthora ramorum* using surface-enhanced Raman spectroscopy†

Sezin Yüksel,‡[a,b,c] Lydia Schwenkbier,‡[a,b,c] Sibyll Pollok,[a,d] Karina Weber,*[a,b,c] Dana Cialla-May*[a,b,c] and Jürgen Popp[a,b,c]

Received 9th June 2015,
Accepted 3rd September 2015

DOI: 10.1039/c5an01156f

www.rsc.org/analyst

In this study, we report on a novel approach for the label-free and species-specific detection of the plant pathogen *Phytophthora ramorum* from real samples using surface enhanced Raman scattering (SERS). In this context, we consider the entire analysis chain including sample preparation, DNA isolation, amplification and hybridization on SERS substrate-immobilized adenine-free capture probes. Thus, the SERS-based detection of target DNA is verified by the strong spectral feature of adenine which indicates the presence of hybridized target DNA. This property was realized by replacing adenine moieties in the species-specific capture probes with 2-aminopurine. In the case of the matching capture and target sequence, the characteristic adenine peak serves as an indicator for specific DNA hybridization. Altogether, this is the first assay demonstrating the detection of a plant pathogen from an infected plant material by label-free SERS employing DNA hybridization on planar SERS substrates consisting of silver nanoparticles.

Introduction

In recent decades a vast number of invasive plant pathogens have spread across European and North American countries. Members of the genus *Phytophthora* are among these. They belong to the most important and aggressive plant pathogens worldwide and pose serious threats to plants in natural and landscaped environments as well as in plant cultivation.[1] One prominent species is *Phytophthora ramorum*[2] which is responsible for the dramatic die back of oaks in North America (sudden oak death) and the *Larix* decline in the United Kingdom.[3] In order to prevent the spread of this pathogen across borders, its reliable and specific detection is mandatory. To date *Phytophthora* diagnosis has been mainly realized by microbiological or PCR-based techniques.[4–8] However, its specific and reliable detection directly in the field from real samples and without much effort remains an on-going challenge. In this context, DNA hybridization assays have been developed which are based on the immobilization of specific capture probes and their interaction with complementary target sequences.[9,10] DNA hybridization can be detected by fluorescent dyes, radioactivity or enzyme induced color changes.[11–13] Recently, surface enhanced Raman spectroscopy (SERS) was highlighted as an attractive analytical tool for the identification of molecular interactions. In terms of high sensitivity and cost effectiveness, it represents an emerging and promising field in bioanalytical research.[14–17] While applying SERS, it is important to consider the interaction between light and molecules as well as metallic nanostructures. The latter are eminent for the amplification of the Raman signal,[18,19] which is increased by several orders of magnitude.[20,21] Thus, SERS combines high molecular specificity, attributed to the Raman effect, with a high sensitivity.[22–24] Therefore it is an excellent tool for both quantitative and qualitative analysis, offering almost unlimited possibilities for multiplexing.[25–27] Moreover, SERS-based DNA detection provides several advantages compared to classical fluorescence techniques. Fluorescence detection requires expensive dyes and complex conjugation chemistry, resulting in a limited number of specific labels. The SERS approach enables the selection of various Raman labels, without bleaching or quenching problems.[28] Furthermore, short data processing times point to the direction of implementing SERS in the development of

[a]*Leibniz Institute of Photonic Technology Jena (IPHT), Albert-Einstein-Straße 9, 07745 Jena, Germany. E-mail: karina.weber@ipht-jena.de; Tel: +49 (0)3641-948390*
[b]*Friedrich Schiller University Jena, Institute of Physical Chemistry and Abbe Center of Photonics, Helmholtzweg 4, 07743 Jena, Germany.*
E-mail: dana.cialla-may@uni-jena.de; Tel: +49 (0)3641-206309
[c]*InfectoGnostics Forschungscampus Jena, Zentrum für Angewandte Forschung, Philosophenweg 7, 07743 Jena, Germany*
[d]*Ernst-Abbe-Hochschule Jena, University of Applied Sciences, Carl-Zeiss-Promenade 2, 07745 Jena, Germany*

†Electronic supplementary information (ESI) available. See DOI: 10.1039/c5an01156f

‡Both authors contributed equally to the paper.

This journal is © The Royal Society of Chemistry 2015

Open Access Article. Published on 04 September 2015. Downloaded on 10/28/2025 2:43:01 AM.
This article is licensed under a Creative Commons Attribution-NonCommercial 3.0 Unported Licence.

rapid and low-cost detection platforms for pathogen diagnosis.[14]

In the last few decades a wide range of SERS-based DNA hybridization assays have been explored. Commonly, the hybridization between specific capture probes and the corresponding target molecules is indicated by a change in the signal of the dye label.[27,29–39] More recently, an elegant label-free detection scheme for specific DNA hybridization was introduced by Halas and co-workers.[40] Usually the DNA spectrum is represented by the four nucleobases: adenine (A), guanine (G), cytosine (C) and thymine (T). Adenine exhibits a more prominent Raman profile than the other nucleobases and strongly dominates the SERS spectra of DNA.[33,41,42] Thus, the adenine signal can serve as an endogenous marker for SERS-based DNA detection. However, in general both capture probes and target sequences consist of multiple adenine moieties, which hamper the SERS-based detection of DNA hybridization. This drawback was circumvented by the substitution of adenine by 2-aminopurine (2-AP) in order to generate adenine-free capture probes.[40] 2-AP serves as an adenine analogue or isomer, exhibiting identical hybridization characteristics.[43–45] It forms a canonical Watson–Crick base pair with thymine and enables the study of nucleic acid structures and their dynamics. Thus, only the SERS spectra of the hybridized target DNA, containing adenine in the sequence, provide the related adenine characteristics. Inspired by this unique feature, we expanded the principle of label-free SERS-based detection to *Phytophthora ramorum* plant pathogens in infected *Rhododendron* leaves. This illustrates, to the best of our knowledge for the first time, the application of label-free SERS towards PCR products from real samples. To this end, we considered a combination of plant sampling, DNA isolation, amplification, hybridization and SERS-based DNA detection to reflect the complete analysis chain.

Experimental section

Plant infection and DNA extraction of *Phytophthora ramorum*

The genomic DNA (gDNA) of *P. ramorum* BBA9/95 was extracted from artificially infected *Rhododendron* leaves (see detached leaf assay, described in detail elsewhere[46]) by homogenizing the samples with a mortar and pestle.[9] The lysate was placed into a micro reaction tube and DNA extraction was performed using the magnetic bead based innuPREP MP Basic Kit according to the recommendations of the manufacturer (Analytik Jena AG, Jena, Germany).

Amplification of target DNA by PCR

Linear-after-the-exponential polymerase chain reaction (LATE-PCR) was carried out to amplify a fragment within the yeast GTP-binding protein (*Ypt*1) target gene region. The conditions for LATE-PCR are described elsewhere[10] (Table 1). DNA of inoculated *Rhododendron* leaves was used in a concentration of 50 ng per reaction. The amplified *Ypt*1-fragments had a length of approximately 450 bp.

SERS substrate preparation

As the SERS substrate, we applied enzymatically generated silver nanoparticles (EGNPs). In extensive studies they were proven as low-cost, highly reproducible and stable bottom-up SERS active substrates.[47,48]

These nanoparticles were generated by an enzyme-induced growth process on glass substrates, described in detail elsewhere.[47] Briefly, a biotin-labeled single-stranded DNA was immobilized onto planar substrates. A streptavidin horseradish peroxidase (HRP) conjugate bound to the biotin and catalyzed the enzymatic generation of nanoparticles from a silver solution. For this purpose the EnzMet™ kit from Nanoprobes Inc., (Yaphank, NY, USA) was used.

Finally, an array of individual EGNP deposits was produced, where closely packed 'desert-rose-like' silver nanostructures with a particle size of approximately 400 nm could be observed (Fig. 1). The strongest electromagnetic field enhancement was located at the sharp and spiky features of the silver intertwined plates.

Scanning electron microscopy (SEM)

The scanning electron microscopy (SEM) images were recorded with a high resolution field emission scanning electron microscope JEOL JSM-6300F (Tokyo, Japan), applying 5 keV accelerating voltage with an accumulation time of 300 s.

Table 1 Primers, capture probes, and single-stranded DNA (ssDNA)

		Sequence 5′–3′	Modification
Capture probes	*P. ramorum*	CCC CCC **A***CT TTC CGT GGG TG**A*** GTT TCC TTT	5′-SH internal 2-AP
	P. lateralis	CGG G**A***G **A***TT TTT TCC CGC TTT CCT TGG GGT **A***A*G	5′-SH internal 2-AP
Primers	YPh1F_LATE	CAT CTC GAC CAT KGG TGT GGA CTT T	w/o
	YPh2R	ACG TTC TCM CAG GCG TAT CT	
ssDNA complementary to *P. ramorum*	*P. ramorum*	AAA GGA AAC TCA CCC ACG GAA AGT GGG GGG	w/o (SERS) 5′-FITC (fluorescence)

A* indicates the substitution of adenine by 2-aminopurine.

Open Access Article. Published on 04 September 2015. Downloaded on 10/28/2025 2:43:01 AM.
This article is licensed under a Creative Commons Attribution-NonCommercial 3.0 Unported Licence.

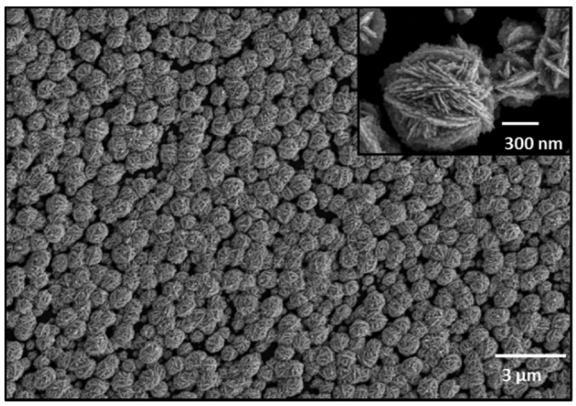

Fig. 1 SEM image of EGNPs. High-resolution scanning electron microscopy (SEM) image of closely packed EGNPs, having a particle size around 400 nm with sharp and spiky features of the EGNPs (*cf.* zoomed image).

For either fluorescence or SERS-based detection, the capture probes were immobilized in triplicate directly on top of the EGNP array *via* their thiol groups (Fig. 2). Thereto they were dissolved in 5× PBS buffer to a final concentration of 20 µM and spotted on the EGNPs with a Nanoplotter 2.1 (GeSim, Germany). After UV-linking at 254 nm for 5 min the substrates were washed with 1× PBS for 2 min. A 0.5% (w/v) solution of bovine serum albumin (BSA) (Carl Roth, Karlsruhe, Germany) in 1× PBST was used to block unspecific binding sites. For the DNA hybridization either 20 µl of the LATE-PCR product or 1 µM of complementary ssDNA (Table 1) were dissolved in 3 × SSC/0.5% SDS and incubated on the substrates for two hours at 58 °C in a humidity chamber. The subsequent washing steps were performed at room temperature (2 × SSC/0.1% SDS, 0.2 × SSC and finally with 0.1 × SSC, 5 min each). Afterwards, fluorescence or SERS detection was performed.

Immobilization of adenine-free capture probes and DNA hybridization on EGNP array

The capture probes, primers and complementary ssDNA were purchased from Eurofins MWG Operon (Ebersberg, Germany; Table 1).

Fluorescence microscopy

Fluorescence images were recorded with the light microscope Axio Imager Z1 (Carl Zeiss Jena GmbH, Jena, Germany). The samples were measured using a 20× objective with an exposure time of 435 ms.

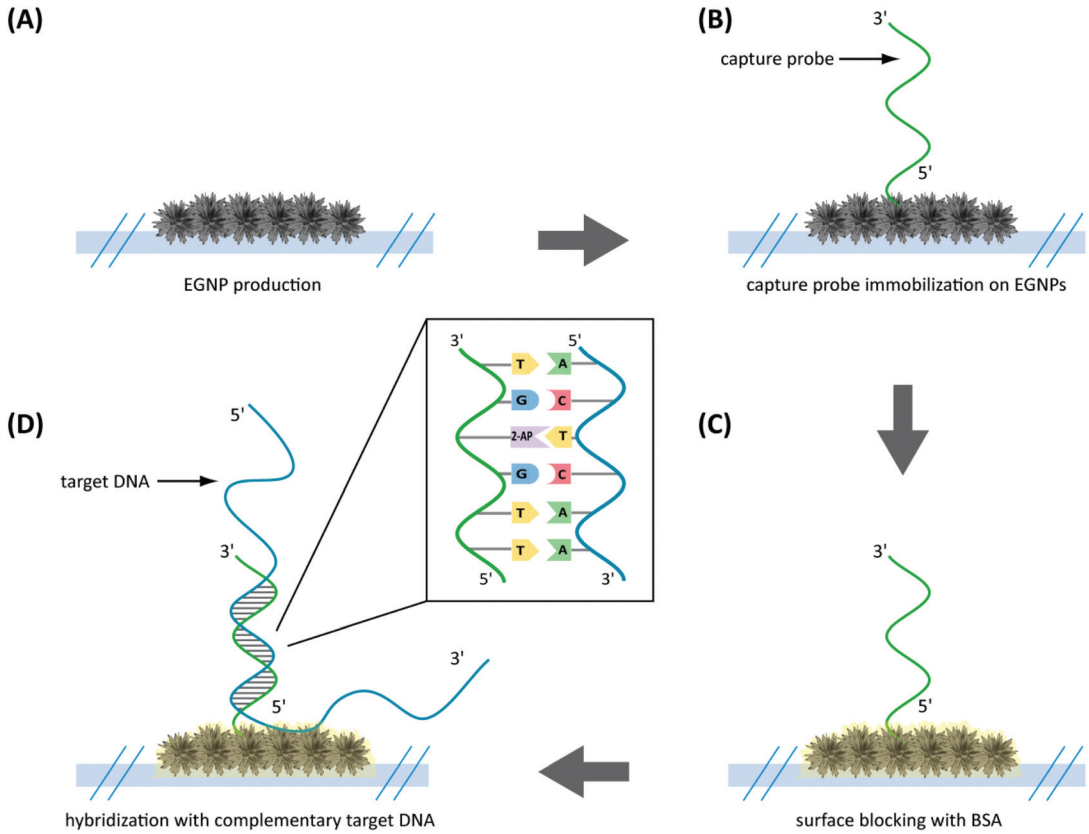

Fig. 2 Schematic illustration of specific DNA hybridization on EGNP immobilized adenine-free capture probes. (A) EGNPs were produced on planar glass substrates. (B) Species-specific capture probes containing 2-aminopurine instead of adenine were immobilized on the EGNP array. (C) DNA-free positions were blocked with BSA. (D) Hybridization of the complementary target DNA (adenine within sequence) was performed.

 This journal is © The Royal Society of Chemistry 2015

Open Access Article. Published on 04 September 2015. Downloaded on 10/28/2025 2:43:01 AM.
This article is licensed under a Creative Commons Attribution-NonCommercial 3.0 Unported Licence.

SERS

SERS spectra were recorded using a confocal Raman microscope (WITec GmbH, Ulm, Germany) equipped with a 488 nm excitation laser line. For the irradiation of the samples a 100× Olympus objective (NA 0.9) with a laser power of 35 μW was employed. The same objective was applied for recording the backscattered light with a spectrometer, equipped with 600 lines per mm grating and a 1024 × 127 pixel CCD camera cooled to 208 K. Average SERS spectra were calculated from ten different measurement points with an integration time of 10 s.

Results and discussion

The study focused on the reliable and label-free detection of *P. ramorum* plant pathogen from infected *Rhododendron* leaves. We applied a label-free SERS-based detection approach to record the specific DNA interaction on a planar SERS substrate (Fig. 3). The assay started with the sampling of the infected plant material and the isolation of pathogenic gDNA, which was used as a template for the amplification of the *Ypt*1 target region by LATE-PCR. This target DNA was then used for hybridization with immobilized capture probes that possessed 2-AP instead of adenine on the EGNP array. Thus, we took advantage of the strong spectral feature of adenine in the SERS spectrum of the target DNA. The presence of adenine exclusively in the target DNA sequence served as an endogenous marker for the label-free SERS-based detection of the hybridization event. Furthermore, the entire analysis chain was considered in order to prove the near-future application of SERS for implementation in an on-site detection system.

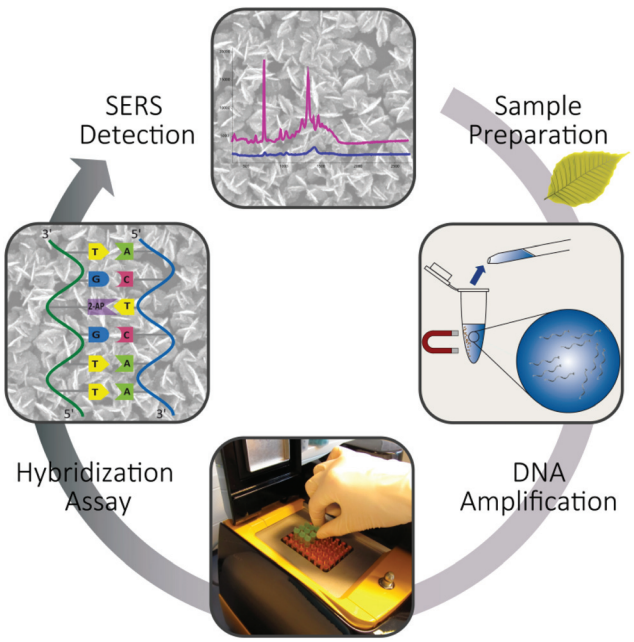

Fig. 3 Label-free SERS-based detection of *P. ramorum*. DNA-based detection of *Phytophthora ramorum* by SERS covering the whole analysis chain. Sample preparation was realized using a mortar and pestle followed by magnetic bead based gDNA isolation, DNA amplification by LATE-PCR and the subsequent hybridization was followed by label-free SERS detection of the molecular DNA–DNA interaction.

DNA isolation and amplification

The preparation of the samples is the first critical step in the successful detection of pathogens. As an example for a proof-of-concept analysis we chose *Rhododendron* leaves of *P. ramorum*-infected plants. The DNA extraction was performed by combining a mortar and pestle for effective cell disruption in conjunction with nucleic acid release.[9,49] This manually operated homogenization is applicable for softer tissues such as *Rhododendron* leaves and provided an incredibly facile way to release gDNA from the plant material. Subsequently, magnetic particle-based DNA isolation enabled easy handling as well as short processing times. Thus, the first step of DNA extraction and purification was realized in a straightforward manner for a potential field application.

LATE-PCR allowed the amplification of the yeast GTP-binding protein (*Ypt*1) target gene of *P. ramorum*. This particular region is located within a single-copy gene, which implies the presence of only one copy per genome. Therefore, a prior DNA amplification was mandatory for proper detection. Accordingly, LATE-PCR was carried out to generate sufficient amounts of single-stranded target DNA.[10] The successful generation of ssDNA was indicated by the appearance of two bands in the analytical gel. The faster migrating DNA represented single-stranded DNA (450 nt) and the higher molecular weight band of 450 bp was double-stranded (see ESI Fig. S1†). By applying asymmetric PCR post-amplification treatment could be omitted.

Fluorescence microscopic detection of target DNA hybridization

In order to verify the functionality of the hybridization assay on the SERS substrate, fluorescence microscopy was performed as a reference method. For this purpose two different capture probes, one for the target species *P. ramorum* (Fig. 4A) and one for the closely related species *P. lateralis* (Fig. 4B), were immobilized on the corresponding EGNP spots. Moreover, EGNPs without any capture probes were analyzed after identical processing steps for blocking, hybridization and washing (Fig. 4C).

Subsequently, hybridization was accomplished using FITC-labeled single-stranded target DNA of *P. ramorum* with a length of 30 nucleotides (Table 1). The selection of this particular *Phytophthora* species relied upon previous studies which focused on the specificity and sensitivity of the *Ypt*1 target gene region.[46] The highest signals were recorded for *P. ramorum*-specific capture probes that entirely matched the target DNA sequence (Fig. 4A). In contrast, only weak signals were detected for the *P. lateralis* capture probes (Fig. 4B). In comparison with the background fluorescence (Fig. 4C) those signals were negligible. Consequently, the functionality of the hybridization assay for the specific detection of *P. ramorum* is

Open Access Article. Published on 04 September 2015. Downloaded on 10/28/2025 2:43:01 AM.
This article is licensed under a Creative Commons Attribution-NonCommercial 3.0 Unported Licence.

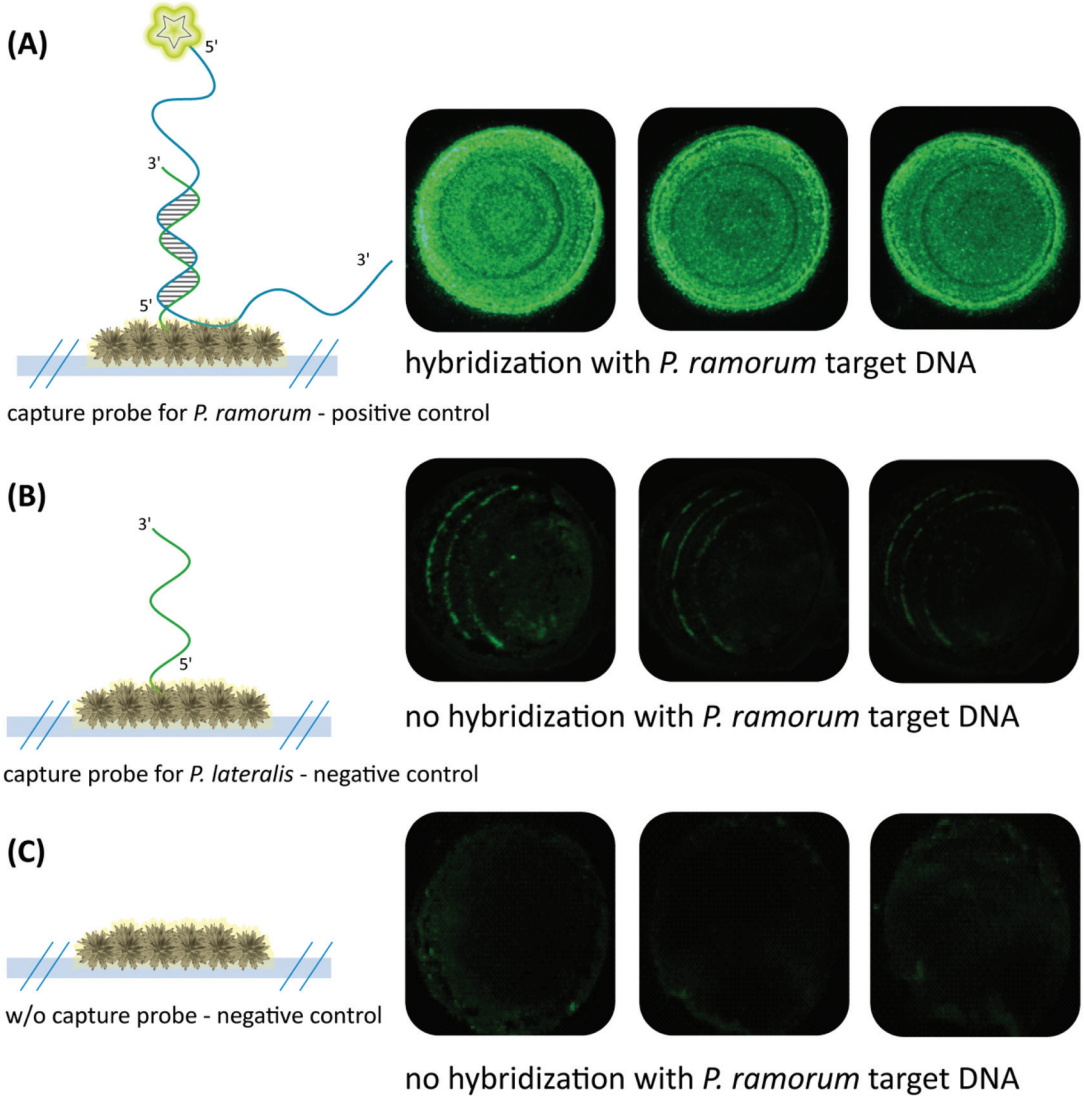

Fig. 4 Fluorescence microscopy to verify the functionality of the hybridization assay on the SERS substrate. (A) Specific hybridization signals (FITC fluorescence) for *P. ramorum* target DNA with matching *P. ramorum* capture probes. (B) Absence of hybridization signals for *P. ramorum* target DNA with non-matching *P. lateralis* capture probes. (C) Background signals of EGNPs. The respective fluorescence signals were depicted as triplicates.

proven. The adenine isomer, 2-AP, in the capture probes exhibited the same hybridization characteristics.

SERS detection of target DNA hybridization

In the next step, the label-free SERS detection of *P. ramorum* DNA was investigated. First, DNA hybridization was accomplished using a short single-stranded target DNA of *P. ramorum* with a length of 30 nucleotides. After that we applied the PCR product isolated from real plant samples and recorded the corresponding SERS spectra.

Hybridization experiments were performed with the 30 nucleotide single-stranded target DNA of *P. ramorum*. Two different adenine-free capture probes, one for the target species *P. ramorum* and one for the non-target species *P. lateralis* were immobilized on the SERS substrate and hybridization was conducted. In Fig. 5, the respective SERS spectra of the hybridized *P. ramorum* capture probes (indicated by a red line), the *P. lateralis* capture probes (indicated by a black line) and the background of the SERS substrate (indicated by a grey line) are displayed as mean values. In the recorded spectra for *P. ramorum* and *P. lateralis* capture probes, the broad carbon spectra are visible between 1200 and 1600 cm^{-1}. This burning effect of the surface is caused by an enhanced electromagnetic field due to applying a relatively long exposure time. Owing to the high carbon background, the Raman vibrational modes of cytosine and adenine were barely detectable between 1200 and 1600 cm^{-1}. In the SERS spectra of *P. ramorum*, where hybridization with the target DNA occurred (see Fig. 5A, red line), one characteristic band of ν(C–C) for cytosine at 1420 cm^{-1} could be observed.[41,50] Moreover, the vibrational modes of guanine

 This journal is © The Royal Society of Chemistry 2015

Open Access Article. Published on 04 September 2015. Downloaded on 10/28/2025 2:43:01 AM.
This article is licensed under a Creative Commons Attribution-NonCommercial 3.0 Unported Licence.

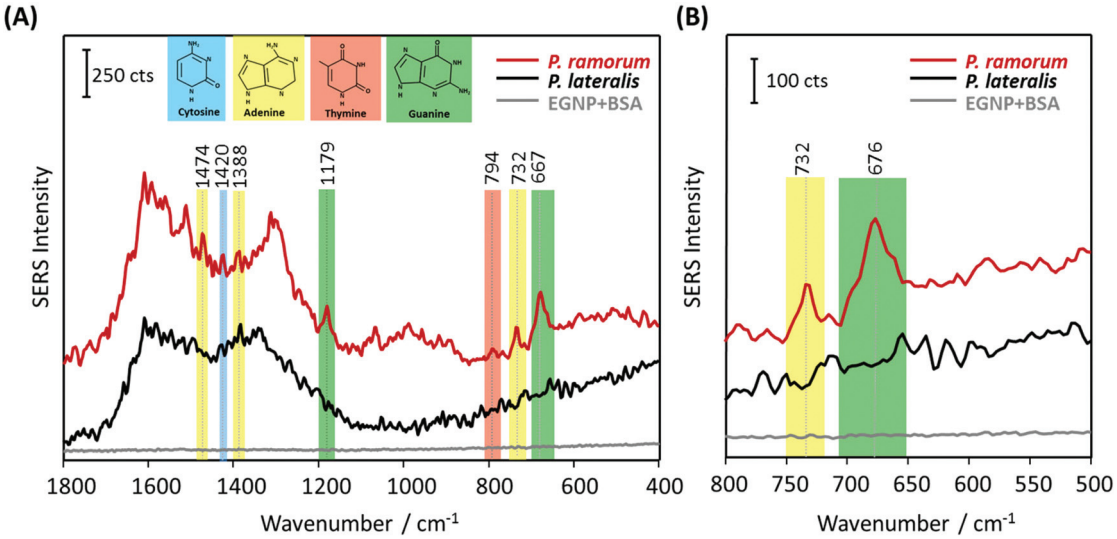

Fig. 5 SERS-based label-free detection of *P. ramorum* target DNA (30 nucleotides) based on adenine-free capture probes. (A) *P. ramorum* capture probes hybridized with complementary target DNA of 30 nucleotides (red line), *P. lateralis* capture probes with no hybridization (black line) and background of the SERS substrate blocked with BSA (grey line). (B) Zoomed view of the spectral range between 500–800 cm^{-1}.

at 1179 cm^{-1} and 667 cm^{-1} were assigned to the ν(C–C) and ring breathing vibrations. The typical Raman bands of adenine were marked with yellow colored frames. The two Raman modes of adenine at 1474 cm^{-1} and 1388 cm^{-1} are referred to as ν(C–N) and ν(C=N) stretching modes respectively. Additionally, the most prominent peak of adenine at 732 cm^{-1} is related to the aromatic ring breathing. Fig. 5B shows the spectral zoom of the region of interest between 500 and 800 cm^{-1}. Accordingly, *P. ramorum* (Fig. 5B, red line) was identified by the dominant peak of adenine at 732 cm^{-1}. In contrast, the SERS spectra of the non-target species *P. lateralis* do not show any characteristic adenine-related modes, indicating that no hybridization occurred (Fig. 5B, black line). Thus, the specific binding of the *P. ramorum* target DNA to the matching capture probe was monitored by the presence of adenine.

In order to demonstrate the applicability of the label-free technique for bioanalytical purposes in terms of pathogen detection, we adapted the SERS approach for DNA isolated from real plant samples, infected with the pathogen *P. ramorum*. The implementation of SERS as a novel tool for pathogen detection resulted in a plethora of publications in the last few years. However, the main challenge of this promising technique is the confirmation of its applicability for on-site use with real samples, *e.g.* from infected plant tissue. Therefore, the main objective of the present study was to demonstrate the application of label-free SERS detection for the plant pathogen DNA, extracted from *Phytophthora* infected *Rhododendron* leaves. Fig. 6 displays the mean SERS spectra of the DNA-hybrid between *P. ramorum*-specific capture probes and *P. ramorum* target DNA, which was amplified by PCR as 450 nucleotide fragments (indicated by a red line), the non-target *P. lateralis* (black line) and the background of the SERS substrate (grey line). In accordance with the findings for the short target DNA fragment, typical vibrational bands at 1081 cm^{-1} and 668 cm^{-1} were observed for guanine in the SERS spectra of *P. ramorum* (see Fig. 6A, red line). Also the less strong Raman bands of thymine at 1234 cm^{-1} and cytosine at 1292 cm^{-1} were depicted in the SERS spectra of the target DNA. However, focusing on adenine as the endogenous marker, very dominant Raman modes at 1384 cm^{-1} and 732 cm^{-1} were monitored for the DNA extracted and amplified from the infected *Rhododendron*. Moreover, the characteristic Raman mode of adenine at 1336 cm^{-1} could be detected due to the presence of a higher amount of the respective nucleobase in the target DNA strand. Similar to previous results the dominant peak at 732 cm^{-1} indicating the presence of adenine served as a significant marker band in comparison with the non-target *P. lateralis* (see Fig. 6B). Altogether, by substituting adenine with 2-AP in the capture probes, the specific hybridization of the *P. ramorum* target DNA could be successfully monitored even while applying this very long PCR product. A proper discrimination between *P. ramorum* (target) and *P. lateralis* (non-target) is possible. Thus, the label-free SERS detection of DNA was exemplarily demonstrated for the important plant pathogen *P. ramorum*.

Reproducibility of the SERS spectra

Despite the fact that SERS-based DNA detection offers great potential regarding a higher sensitivity and specificity, it is still in competition with more common techniques such as fluorescence spectroscopy. One drawback for SERS measurements is the lack of good spectral reproducibility as well as precise batch-to-batch and day-to-day recordings. For this reason the current study also addressed the batch-to-batch reproducibility of the SERS signals occurring in the case of DNA hybridization. Independent experiments were performed

Open Access Article. Published on 04 September 2015. Downloaded on 10/28/2025 2:43:01 AM.
This article is licensed under a Creative Commons Attribution-NonCommercial 3.0 Unported Licence.

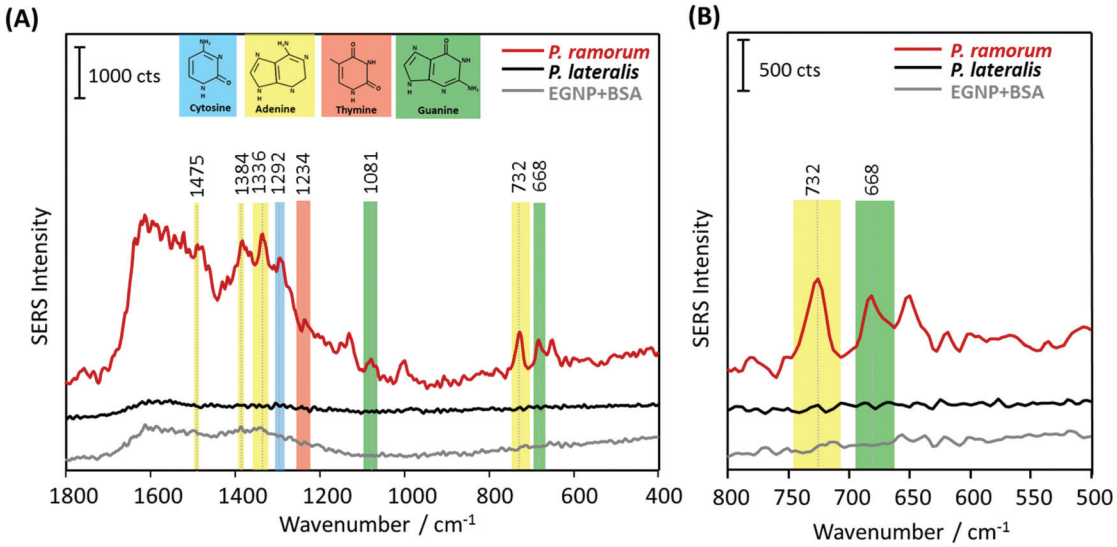

Fig. 6 SERS-based label-free detection of *P. ramorum* target DNA (450 nucleotide PCR product) based on adenine-free capture probes. (A) *P. ramorum* capture probes hybridized with the complementary target DNA of 450 nucleotide PCR product (red line), *P. lateralis* capture probes with no hybridization (black line) and background of the SERS substrate blocked with BSA (grey line). (B) Zoomed view of the spectral range between 500–800 cm^{-1}.

using various DNA extracts, conducting individual PCR runs and hybridization assays. Fig. 7 depicts the normalized integrated SERS intensity for various batches. The adenine peak at 732 cm^{-1} was integrated for the SERS spectra of the matching target (*P. ramorum*), the non-matching control (*P. lateralis*) and the background of the SERS substrate and then normalized to the peak of the highest intensity. In comparison with the capture probes and the background, the integrated SERS intensity at 732 cm^{-1} showed the highest values, having a relative standard deviation (RSD) around 40% (see Fig. 7). The high relative standard deviation can be explained by the different orientations of the DNA on the metallic surface and by an inhomogeneous coverage of BSA on silver nanoparticles. Due to the surface blocking, the SERS intensity can vary during point-to-point measurements. Hence, the results are not sufficient for quantitative detection. However, monitoring the DNA hybridization event without employing labels in SERS based detection is demonstrated. It is clearly visible that the presence of adenine in the SERS spectra of the target DNA served as an indicator for the DNA hybridization.

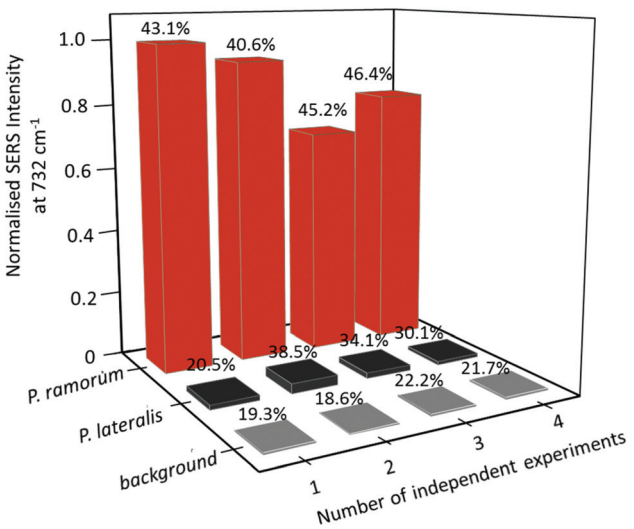

Fig. 7 Spectral reproducibility considering independent experiments. Discrimination between positive (red columns – *P. ramorum*) and negative hybridization signals (black columns – *P. lateralis*, grey columns – EGNP background) generated for AP-2 capture probes. The standard deviation is illustrated by the percentage values.

Conclusions and outlook

In recent years, SERS has been applied for a variety of analyses in the life science sector. Due to its high sensitivity and specificity, it offers great potential for the development of novel biosensors. In this study we expanded its application for the label-free detection of important plant pathogens using the example of *Phytophthora ramorum*. To the best of our knowledge, this is the first report on the label-free detection of the PCR product, isolated from infected plant tissue. Here, DNA-based detection of *P. ramorum* was achieved by covering the whole analytical chain. The sample preparation was realized by an easy tissue disruption procedure combined with magnetic bead-based nucleic acid isolation. The subsequent DNA amplification was performed by LATE-PCR, which enabled the generation of single-stranded target DNA. Thus, a post-PCR processing step for the generation of ssDNA could be omitted. In order to improve the detection and achieve a putative in-

 This journal is © The Royal Society of Chemistry 2015

Open Access Article. Published on 04 September 2015. Downloaded on 10/28/2025 2:43:01 AM.
This article is licensed under a Creative Commons Attribution-NonCommercial 3.0 Unported Licence.

field application, novel isothermal amplification techniques could be implemented.[51,52] Moreover, the SERS-based DNA detection, relying on DNA–DNA-hybrid formation, could be performed in a handheld Raman device, that allows the applicability at the point-of-need due to its portability.

In summary, a reliable, reproducible and thermally stable SERS assay has been developed for the detection of specific DNA hybridization between immobilized capture probes and the sequence-matching target DNA. We have highlighted the application of SERS to identify the adenine-containing target DNA isolated and amplified from infected *Rhododendron* leaves, in conjunction with adenine-free capture probes.

Acknowledgements

We thank Stephan König and Sabine Werres from the Julius Kühn–Institute Braunschweig, Germany for capture probe design, preparation of artificially inoculated *Rhododendron* leaves and extraction and reprocessing of the *Phytophthora* DNA. The project "PhytoChip-Validierung" (28-1-54.081-10) is financed by the Federal Ministry of Food and Agriculture (BMEL) based on a decision of the Parliament of the Federal Republic of Germany *via* the Federal Office for Agriculture and Food (BLE) under the innovation support program. Funding of the project "JBCI 2.0" (03IPT513Y) within the framework "InnoProfile Transfer – Unternehmen Region", the Federal Ministry of Education and Research, Germany (BMBF) is gratefully acknowledged.

References

1 O. K. Ribeiro and K. Lamour, *Phytophthora: Global Perspect.*, 2013, **2**, 1.
2 S. Werres, R. Marwitz, W. Veld, A. De Cock, P. J. M. Bonants, M. De Weerdt, K. Themann, E. Ilieva and R. P. Baayen, *Mycol. Res.*, 2001, **105**, 1155–1165.
3 C. Brasier and J. Webber, *Nature*, 2010, **466**, 824–825.
4 G. J. Bilodeau, C. A. Levesque, A. W. A. M. de Cock, C. Duchaine, S. Briere, P. Uribe, F. N. Martin and R. C. Hamelin, *Phytopathology*, 2007, **97**, 632–642.
5 F. N. Martin, *Phytophthora: Global Perspect.*, 2013, **2**, 19.
6 P. A. O'Brien, N. Williams and G. E. S. Hardy, *Crit. Rev. Microbiol.*, 2009, **35**, 169–181.
7 L. Schena and D. E. L. Cooke, *J. Microbiol. Methods*, 2006, **67**, 70–85.
8 L. Schena, J. M. Duncan and D. E. L. Cooke, *Plant Pathol.*, 2008, **57**, 64–75.
9 S. Julich, M. Riedel, M. Kielpinski, M. Urban, R. Kretschmer, S. Wagner, W. Fritzsche, T. Henkel, R. Moeller and S. Werres, *Biosens. Bioelectron.*, 2011, **26**, 4070–4075.
10 L. Schwenkbier, S. Koenig, S. Wagner, S. Pollok, J. Weber, M. Hentschel, J. Popp, S. Werres and K. Weber, *Microchim. Acta*, 2014, **181**, 1669–1679.
11 D. Cialla, K. Weber, R. Boehme, U. Huebner, H. Schneidewind, M. Zeisberger, R. Mattheis, R. Moeller and J. Popp, *Beilstein J. Nanotechnol.*, 2011, **2**, 501–508.
12 M. R. Hartman, R. C. H. Ruiz, S. Hamada, C. Xu, K. G. Yancey, Y. Yu, W. Han and D. Luo, *Nanoscale*, 2013, **5**, 10141–10154.
13 G. M. Santos, F. Zhao, J. Zeng, M. Li and W. C. Shih, *J. Biophotonics*, 2015, 9999.
14 D. Cialla, S. Pollok, C. Steinbruecker, K. Weber and J. Popp, *Nanophotonics*, 2014, **3**, 383–411.
15 X. Guo, *J. Biophotonics*, 2012, **5**, 483–501.
16 S. Mahajan, J. Richardson, T. Brown and P. N. Bartlett, *J. Am. Chem. Soc.*, 2008, **130**, 15589–15601.
17 T. Vo-Dinh, H.-N. Wang and J. Scaffidi, *J. Biophotonics*, 2010, **3**, 89–102.
18 M. Baia, L. Baia, S. Astilean and J. Popp, *Appl. Phys. Lett.*, 2006, 88.
19 S. Schluecker, *Angew. Chem., Int. Ed.*, 2014, **53**, 4756–4795.
20 E. C. Le Ru and P. G. Etchegoin, *Annu. Rev. Phys. Chem.*, 2012, **63**, 65–87.
21 M. Moskovits, *J. Raman Spectrosc.*, 2005, **36**, 485–496.
22 D. Cialla, U. Huebner, H. Schneidewind, R. Moeller and J. Popp, *ChemPhysChem*, 2008, **9**, 758–762.
23 K. K. Hering, R. Moeller, W. Fritzsche and J. Popp, *ChemPhysChem*, 2008, **9**, 867–872.
24 N. Pavillon, K. Bando, K. Fujita and N. I. Smith, *J. Biophotonics*, 2013, **6**, 587–597.
25 Y. Lai, S. Sun, T. He, S. Schlucker and Y. Wang, *RSC Adv.*, 2015, **5**, 13762–13767.
26 S. Niebling, H. Y. Kuchelmeister, C. Schmuck and S. Schluecker, *Chem. Sci.*, 2012, **3**, 3371–3377.
27 K. K. Strelau, A. Brinker, C. Schnee, K. Weber, R. Moeller and J. Popp, *J. Raman Spectrosc.*, 2011, **42**, 243–250.
28 A. J. Driscoll, M. H. Harpster and P. A. Johnson, *Phys. Chem. Chem. Phys.*, 2013, **15**, 20415–20433.
29 J. L. Abell, J. M. Garren, J. D. Driskell, R. A. Tripp and Y. Zhao, *J. Am. Chem. Soc.*, 2012, **134**, 12889–12892.
30 K. Faulds, W. E. Smith and D. Graham, *Analyst*, 2005, **130**, 1125–1131.
31 K. Gracie, E. Correa, S. Mabbott, J. A. Dougan, D. Graham, R. Goodacre and K. Faulds, *Chem. Sci.*, 2014, **5**, 1030–1040.
32 D. Graham, B. J. Mallinder, D. Whitecombe, N. D. Watson and W. E. Smith, *Anal. Chem.*, 2002, **74**, 1069–1074.
33 M. Green, F. M. Liu, L. Cohen, P. Kollensperger and T. Cass, *Faraday Discuss.*, 2006, **132**, 269–280.
34 Y. Lu, Q. Huang, G. Meng, L. Wu and J. Zhang, *Analyst*, 2014, **139**, 3083–3087.
35 N. E. Marotta, K. R. Beavers and L. A. Bottomley, *Anal. Chem.*, 2013, **85**, 1440–1446.
36 C. M. Muntean, N. Leopold, A. Halmagyi and S. Valimareanu, *J. Raman Spectrosc.*, 2011, **42**, 844–850.
37 H. T. Ngo, H.-N. Wang, A. M. Fales, B. P. Nicholson, C. W. Woods and T. Vo-Dinh, *Analyst*, 2014, **139**, 5655–5659.
38 E. Papadopoulou and S. E. J. Bell, *Chem. Commun.*, 2011, **47**, 10966–10968.

Open Access Article. Published on 04 September 2015. Downloaded on 10/28/2025 2:43:01 AM.
This article is licensed under a Creative Commons Attribution-NonCommercial 3.0 Unported Licence.

39 D. van Lierop, I. A. Larmour, K. Faulds and D. Graham, *Anal. Chem.*, 2013, **85**, 1408–1414.
40 A. Barhoumi and N. J. Halas, *J. Am. Chem. Soc.*, 2010, **132**, 12792–12793.
41 A. Barhoumi, D. Zhang, F. Tam and N. J. Halas, *J. Am. Chem. Soc.*, 2008, **130**, 5523–5529.
42 C. Otto, F. F. M. Demul, A. Huizinga and J. Greve, *J. Phys. Chem.*, 1988, **92**, 1239–1244.
43 A. Dallmann, L. Dehmel, T. Peters, C. Muegge, C. Griesinger, J. Tuma and N. P. Ernsting, *Angew. Chem., Int. Ed.*, 2010, **49**, 5989–5992.
44 J. M. Jean and K. B. Hall, *Proc. Natl. Acad. Sci. U. S. A.*, 2001, **98**, 37–41.
45 L. C. Sowers, G. V. Fazakerley, R. Eritja, B. E. Kaplan and M. F. Goodman, *Proc. Natl. Acad. Sci. U. S. A.*, 1986, **83**, 5434–5438.
46 S. König, L. Schwenkbier, S. Pollok, M. Riedel, S. Wagner, J. Popp, K. Weber and S. Werres, *Plant Pathol.*, 2015, **64**, 1176–1189.
47 H. Schneidewind, T. Schueler, K. K. Strelau, K. Weber, D. Cialla, M. Diegel, R. Mattheis, A. Berger, R. Moeller and J. Popp, *Beilstein J. Nanotechnol.*, 2012, **3**, 404–414.
48 T. Schueler, A. Steinbrueck, G. Festag, R. Moeller and W. Fritzsche, *J. Nanopart. Res.*, 2009, **11**, 939–946.
49 T. D. Miles, F. N. Martin and M. D. Coffey, *Phytopathology*, 2015, **105**, 265–278.
50 N. H. Jang, *Bull. Korean Chem. Soc.*, 2002, **23**, 1790–1800.
51 L. Schwenkbier, S. Pollok, S. Koenig, M. Urban, S. Werres, D. Cialla-May, K. Weber and J. Popp, *Anal. Methods*, 2015, **7**, 211–217.
52 J. A. Tomlinson, M. J. Dickinson and N. Boonham, *Phytopathology*, 2010, **100**, 143–149.

 This journal is © The Royal Society of Chemistry 2015